Journal of Materials Science: Materials in Electronics (2019) 30:5726–5732
https://doi.org/10.1007/s10854-019-00866-4

Effects of Ca^{2+} substitution on microstructure and microwave dielectric properties of low loss $Ba(Mg_{1/3}Nb_{2/3})O_3$ perovskite ceramics

He Wang[1] · Renli Fu[1] · He Liu[1] · Jun Fang[1] · Guojun Li[1]

Received: 19 December 2018 / Accepted: 30 January 2019 / Published online: 15 February 2019

Abstract
$Ba_{1-x}Ca_x(Mg_{1/3}Nb_{2/3})O_3$ ($0 \le x \le 0.02$) perovskite ceramics were prepared by the solid-state reaction method. The phase composition and microstructure were characterized by XRD and SEM, respectively. The result showed that all ceramics exhibited the 1:2 ordered perovskite structure, and the grain size decreased first and then increased with different substitution amount of Ca^{2+} for Ba^{2+}. The dielectric properties were examined by Vector network analyzer, and the Raman spectra was used to interpret the dielectric properties of $Ba_{1-x}Ca_x(Mg_{1/3}Nb_{2/3})O_3$ ceramics. The dielectric constant (ε_r) were strongly depended on the Raman shift of $A_{1g}(O)$ stretch mode, and the quality factor ($Q \times f$) manifested great correlated with the full width at half maxima (FWHM) of $A_{1g}(O)$ stretch mode. The $Ba_{1-x}Ca_x(Mg_{1/3}Nb_{2/3})O_3$ ceramics substituted of Ca^{2+} for Ba^{2+} in $x = 0.005$, which possessed the narrowest FWHM and the highest degree of 1:2 ordering, showed the best microwave dielectric properties: $\varepsilon_r = 31.64$, $Q \times f = 74421$ GHz, $\tau_f = 14.59$ ppm/°C.

1 Introduction

The remarkable 1:2 ordered perovskite ceramics, such as $Ba(Mg_{1/3}Ta_{2/3})O_3$ [1], $Ba(Zn_{1/3}Ta_{2/3})O_3$ [2] and $Ba(Mg_{1/3}Nb_{2/3})O_3$ [3] and so on, have great potential for microwave communication application. For practical application, such as the filter and resonator, the ceramics are required simultaneous with high quality factor ($Q \times f$), appropriate dielectric constant (ε_r) and near-zero temperature coefficient of resonant frequency (τ_f). The research for these ceramics with high-performance in microwave communication is still in progress, and the key factors influencing on the dielectric properties of ceramics are not well understand. Recently, Raman spectra was found to become one of the useful tools for the analysis of ceramics crystal structure, and the Raman spectra had succeed to be used to interpret the dielectric properties of ceramics [4, 5].

$Ba(Mg_{1/3}Nb_{2/3})O_3$ (hereafter abbreviated as BMN), as a Nb-based perovskite ceramics, is known to possess moderate dielectric constant ε_r (= 32) and high $Q \times f$ value (= 56,000 GHz) [6]. However, the BMN ceramics have a relatively high positive temperature coefficient of resonant frequency τ_f (= 33 ppm/°C), and its quality factor ($Q \times f$) have not run up to the performance levels of the Ta-based perovskite ceramics [7]. In the BMN-type ceramics, two kinds of ordered structures have been found as follows: 1:2 ordered hexagonal structure and 1:1 ordered cubic structure [8], whose difference are closely associated with the arrangement of B-site cations. For the pure BMN, which has a 1:2 ordered hexagonal structure. The previous research of BMN-type ceramics aimed at examining the structure transformation from 1:2 ordered hexagonal structure to 1:1 ordered cubic structure, which could be achieved by modifying the degree of B-site cations ordering through different amounts of A-site or B-site substitutions. Akbas et al. [9] reported that the A-site substitutions of La^{2+} for Ba^{2+} in $Ba_{1-x}La_x[Mg_{(1+x)/3}Nb_{(2-x)/3}]O_3$ ($x = 0$, 0.05, 0.1, 0.15, 0.25, 0.5, 0.75) induced a transformation from 1:2 ordered structure to 1:1 ordered structure, and tuned the τ_f of BMN to a zero value. Zhang et al. [10] discussed the crystal structures of $Ba[Mg_{(1-x)/3}Zr_xNb_{2(1-x)/3}]O_3$ ($x = 0$, 0.05, 0.1, 0.15) by the XRD and Raman spectra, whose results showed that the distortion of oxygen octahedron occurred where x = 0.05, and the ordered phase transformed from 1:2 ordering to 1:1 ordering. In addition, Tian et al. [11] used the B-site substitutions of W^{6+} cation in $BaWO_4$ for Nb^{5+} cation in $Ba(Mg_{1/3}Nb_{2/3})O_3$ enhanced the degree of B-site cation ordering of $Ba(Mg_{1/3}Nb_{2/3})O_3$ and obtained outstanding

✉ Renli Fu
renlifu@nuaa.edu.cn

[1] College of Materials Science and Technology, Nanjing University of Aeronautics and Astronautics, Nanjing 210016, People's Republic of China

microwave dielectric properties: $\varepsilon_r = 32$, $Q \times f = 82{,}300$ GHz and $\tau_f = 28$ ppm/°C. However, the $BaWO_4$ and $Ba_5Nb_4O_{15}$ phases consisted in all ceramics. Bisht et al. [12] investigated the microwave dielectric properties of $(1-x)Ba(Mg_{1/3}Nb_{2/3})O_3 - xBa(Mg_{1/8}Nb_{3/4})O_3$ ($x = 0$, 0.005, 0.01 and 0.02) solid solutions and obtained the maximum $Q \times f$ of 74,000 GHz when $x = 0.005$. Meanwhile, the τ_f reached the minimum value (= 21 ppm/°C) and the Raman spectra was indicative of the presence of 1:2 ordered structure for all ceramics.

In this work, the synthesis of $Ba_{1-x}Ca_x(Mg_{1/3}Nb_{2/3})O_3$ ceramics using a solid-state reaction method was presented, and the substitution amount of Ca^{2+} for Ba^{2+} was designed in the relatively small range of ($x = 0$, 0.005, 0.01, 0.015, 0.02). By these less substitution amount of Ca^{2+} for Ba^{2+}, we expected the $Ba_{1-x}Ca_x(Mg_{1/3}Nb_{2/3})O_3$ ceramics to keep 1:2 ordered structure and not be transformed into 1:1 ordered structure. As we all know, the $Ba(B'_{1/3}B''_{2/3})O_3$ ceramics with 1:2 ordered structure exhibit better $Q \times f$ [13]. In the lattice of BMN ceramics, the 1:2 ordered structure comprises single layers of octahedral B-site Mg^{2+} cations alternating with double layers of Nb^{5+} cations perpendicular to the ⟨111⟩ direction of the cubic subcell, which can be identified by using XRD and Raman spectra [14]. The effect of substitution amount of Ca^{2+} for Ba^{2+} on the phase composition, microstructure and sintered properties of $Ba(Mg_{1/3}Nb_{2/3})O_3$ ceramics were discussed. The dielectric properties of $Ba_{1-x}Ca_x(Mg_{1/3}Nb_{2/3})O_3$ ceramics were examined by Vector network analyzer, and the Raman spectra was used to interpret the dielectric properties, whose results shed light on the correlation between vibration characteristics of ceramics and dielectric properties.

2 Experimental procedure

$Ba_{1-x}Ca_x(Mg_{1/3}Nb_{2/3})O_3$ ceramics ($x = 0$, 0.005, 0.01, 0.015, 0.02) were prepared by the conventional solid-state reaction method. The starting materials $BaCO_3$, $CaCO_3$, MgO and Nb_2O_5 with high-purity grade (> 99%) were purchased from Sinopharm Chemical Reagent Co., Ltd (Shanghai, China). The starting materials were mixed according to the designed composition, then milled in nylon jars with ZrO_2 balls and deionized water for 20 h. After drying, the powders were calcined at 1300 °C for 3 h first. The resulting powders were re-milled for 10 h. After that, the dried and re-milled mixtures were granulated with appropriate poly vinyl alcohol (PVA) as binder. The samples for test were pressed into cylinders ($\Phi 15 \times 7$ mm) under 200 MPa uniaxial pressure, and sintered in air at 1500 °C for 4 h.

The phase of as-prepared samples were indexed by X-ray diffraction (XRD; Bruker D8 Advanced, Germany) using CuKα radiation. Microstructure of the samples were observed by a scanning electron microscopy (SEM; Hitachi-SU8010, Japan). The grain size distribution and the average grain size were calculated by a Nano Measurer software (Fudan University, China), which can count the size and number of different grains in the SEM photographs, and then make the columnar statistical distribution map [15]. The bulk densities of the sintered samples were measured by Archimedes method. Raman spectra were excited with 532 nm He–Ne laser and recorded using a Raman spectrometer (Renishaw InVia, England). The microwave dielectric properties were measured using a Vector network analyzer (Advantest R3767C, Japan) at microwave frequency (~6 GHz), while the Hakki and Coleman's dielectric resonant method was used under TE_{011} and $TE_{01\delta}$ modes [16, 17]. The τ_f values were measured at microwave frequency in the temperature range of 25–85 °C according to the following formula:

$$\tau_f = \frac{f_{80} - f_{25}}{f_{25}(80 - 25)} \tag{1}$$

where f_{25} and f_{80} were the resonant frequencies at 25 and 80 °C, respectively. In BMN-type structure, the degree of ordering was evaluated by calculating the B-site ordered parameter (S) through the XRD, which was defined as follow [18]:

$$S = \sqrt{\frac{\left(\frac{I_{(100)}}{I_{(102),(012),(110)}}\right)_{obsed}}{\left(\frac{I_{(100)}}{I_{(102),(012),(110)}}\right)_{theor}}} \tag{2}$$

where $\left(\frac{I_{(100)}}{I_{(102),(012),(110)}}\right)_{obsed}$ and $\left(\frac{I_{(100)}}{I_{(102),(012),(110)}}\right)_{theor}$ are the intensity ratio of the (100) superlattice diffraction peak to that of ((102), (012), (110)) main diffraction peak from the observed and the theoretical values of complete ordering, respectively. In the BMN ceramics, the value of $\left(\frac{I_{(100)}}{I_{(102),(012),(110)}}\right)_{theor}$ is 3.04% [19].

3 Results and discussion

The results of the crystallographic analyses of $Ba_{1-x}Ca_x(Mg_{1/3}Nb_{2/3})O_3$ ceramics sintered at 1500 °C, are shown in the X-ray diffractograms in Fig. 1. The BMN phase with the perovskite structure was predominantly formed, and all of the peaks were well indexed to the $P\bar{3}m1$ space group of hexagonal structure. The weak peaks located at 17.6° caused by 1:2 ordered superlattice structure could be observed in the part I, which resulted in the splitting in (422) and (226) diffraction peaks as shown in the part II [20]. In addition, being highly sensitive to short-range ordering, Raman spectra succeeded in probing the 1:2 ordering, even

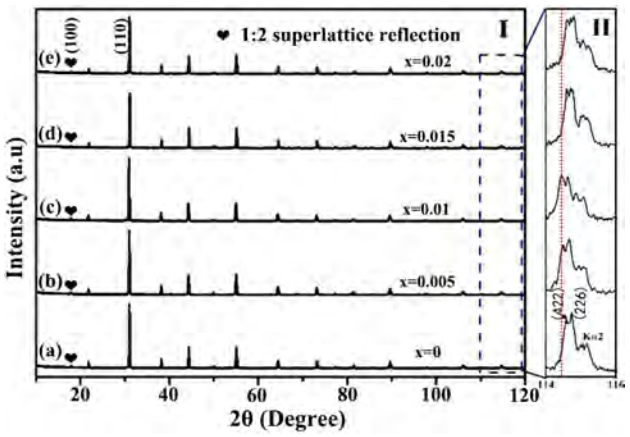

Fig. 1 The XRD patterns of $Ba_{1-x}Ca_x(Mg_{1/3}Nb_{2/3})O_3$ ceramics sintered at 1500 °C

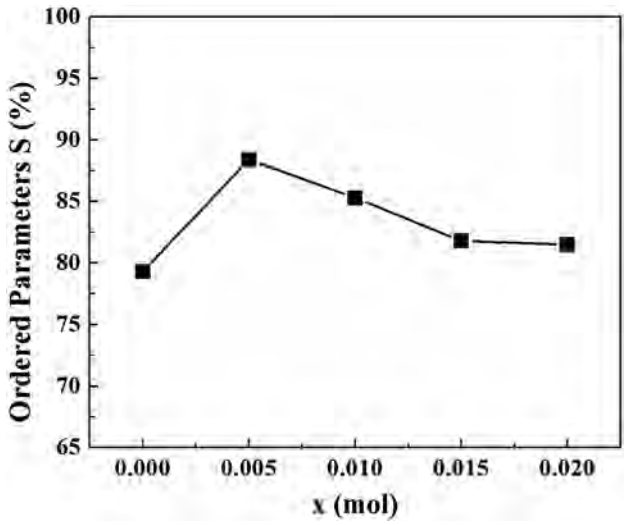

Fig. 2 The ordered parameters S of $Ba_{1-x}Ca_x(Mg_{1/3}Nb_{2/3})O_3$ ceramics sintered at 1500 °C

in the samples in which XRD failed to probe the 1:2 ordering [21]. Furthermore, the (422) diffraction peak shifted to a higher 2θ angle with the increasing of substitution amount of Ca^{2+} for Ba^{2+}, which could be the reason that the ionic radius of Ca^{2+} (1.34 Å) was smaller than Ba^{2+} (1.6 Å) [22], indicating the formation of $Ba_{1-x}Ca_x(Mg_{1/3}Nb_{2/3})O_3$ solid solutions. Table 1 lists the lattice parameters obtained from the refinement of XRD patterns shown in Fig. 1. The cell volume showed the trend of decreasing with the increasing of substitution amount of Ca^{2+} for Ba^{2+}, which was reflected in the shift of the (422) diffraction peak. The ordered parameters S of $Ba_{1-x}Ca_x(Mg_{1/3}Nb_{2/3})O_3$ ceramics sintered at 1500 °C are presented in Fig. 2. Generally, the degree of B-site cations ordering or the degree of lattice distortion had great influenced on the dielectric properties of the ceramics, and the dielectric loss would be decreased with the increasing of degree of lattice distortion [23]. The maximum values of ordered parameters (S = 88.4%) occurred where $x = 0.005$, while the $Ba_{1-x}Ca_x(Mg_{1/3}Nb_{2/3})O_3$ ceramics had the largest $Q \times f$ value.

The SEM photographs of $Ba_{1-x}Ca_x(Mg_{1/3}Nb_{2/3})O_3$ ceramics sintered at 1500 °C are shown in Fig. 3, and the calculated grain size distributions for all SEM photographs are plotted in Fig. 4. Overall, the SEM photographs

Table 1 Lattice parameters obtained from the refinement of XRD patterns shown in Fig. 1

x	a (Å)	c (Å)	$V_{unitcell}$ (Å^3)
0.0	5.7740	7.0941	204.82
0.005	5.7793	7.0956	205.24
0.01	5.7819	7.0941	205.25
0.015	5.7735	7.0925	204.74
0.02	5.7734	7.0893	204.64

revealed the evolution process of grain growth in the $Ba_{1-x}Ca_x(Mg_{1/3}Nb_{2/3})O_3$ ceramics with different substitution amount of Ca^{2+} for Ba^{2+}. The grain size of the $Ba_{1-x}Ca_x(Mg_{1/3}Nb_{2/3})O_3$ ceramics tended to decrease with the increasing of substitution amount of Ca^{2+} for Ba^{2+} in the range of $(0 \le x \le 0.015)$ as shown in Fig. 3a–d, which indicated that a small substitution amount of Ca^{2+} for Ba^{2+} could refine the grain of ceramics by the formation of solid solutions and decreasing the activation energy required for the reaction [24]. However, the grains size became obviously larger when the substitution amount of Ca^{2+} for Ba^{2+} reached $x = 0.02$, as shown in Fig. 3e. It could be the reason that the diffusion rate of Ca^{2+} is much faster than that of Ba^{2+}, as the fact that the Ba atomic weight (137.33 g/mol) is much heavier than the Ca atomic weight (40.08 g/mol), which enhances the sinterability of ceramics when adding a large number substitution amount of Ca^{2+} for Ba^{2+} [25]. The bulk density and relative density of $Ba_{1-x}Ca_x(Mg_{1/3}Nb_{2/3})O_3$ ceramics with different substitution amount of Ca^{2+} for Ba^{2+} sintered at 1500 °C are shown in Fig. 5. The relative density of ceramics were calculated by the ratio of the experimentally measured density to the theoretical one of the sintered ceramics. It was clearly seen that all samples have been sintered compactly and their relative density were above 95%, which was in good agreement with SEM characterization as shown in Fig. 3.

The Raman spectra of $Ba_{1-x}Ca_x(Mg_{1/3}Nb_{2/3})O_3$ ceramics sintered at 1500 °C are shown in Fig. 6. In the Raman spectra, we could observe four prominent peaks as follows: the F_{2g}(Ba) phonon mode near 104 cm^{-1}, the F_{2g}(O) phonon mode near 385 cm^{-1}, the E_g(O) phonon mode near 436 cm^{-1} and the A_{1g}(O) stretch mode near 789 cm^{-1}, which were related to the ordered structure of $Ba_{1-x}Ca_x(Mg_{1/3}Nb_{2/3})$

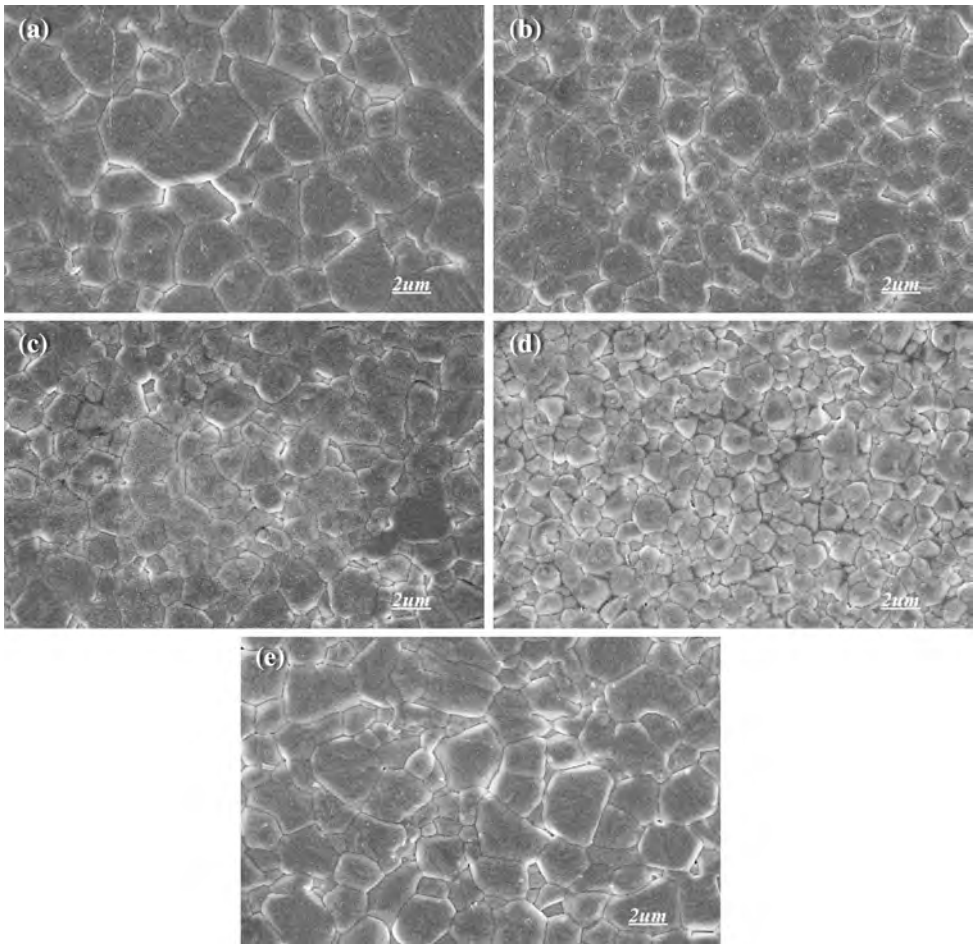

Fig. 3 The SEM images of $Ba_{1-x}Ca_x(Mg_{1/3}Nb_{2/3})O_3$ ceramics sintered at 1500 °C

O_3 ceramics [26]. Among them, the F_{2g}(Ba) phonon mode is superimposed mode of A_{1g}(Ba) and E_g(Ba), while the F_{2g}(O) phonon mode is superimposed mode of A_{1g}(O) and E_g(O). The three weak phonon modes at the 170–300 cm^{-1} range were associated with the E_g(O), E_g(Nb) and A_{1g}(Nb) modes, whose intensities of phonon modes could be used to determine the degree of 1:2 ordering [27]. Furthermore, the A_{1g}(O) stretch mode possessing the strongest energy, could provide important information on the correlation between vibration characteristics of the microwave dielectric ceramics and the dielectric properties [28].

The correlation of dielectric constant with Raman shift of A_{1g}(O) stretch mode of $Ba_{1-x}Ca_x(Mg_{1/3}Nb_{2/3})O_3$ ceramics are illustrated in Fig. 7. It could be seen that the Raman shift kept positive correlation with the dielectric constant with the increasing of substitution amount of Ca^{2+} for Ba^{2+}. The Raman shift was closely related to the rigidity of the oxygen octahedral. For rigid oxygen octahedra, the relative motion of Ba^{2+} cation to NbO_6 anions induced by microwave energy is smaller. A lower Raman shift implied a more rigid oxygen octahedron and a lower polarizability, which resulted in the lower dielectric constant [29]. The correlation of $Q\times f$ value with the FWHM of A_{1g}(O) stretch mode of $Ba_{1-x}Ca_x(Mg_{1/3}Nb_{2/3})O_3$ ceramics are shown in Fig. 8. The FWHM showed the negative correlation with $Q\times f$ value. The large FWHM indicates a poor crystalline structure and a short phonon lifetime [5]. Similarly, the narrowed FWHM of A_{1g}(O) mode indicates the highly ordering and rigid oxygen-cage structure; therefore, the decay time of the propagation of the microwave energy is longer, and this implies the material possesses high $Q\times f$ value. The relationship between $Q\times f$ value and FWHM was reported before by Chen et al. [30].

The variation of τ_f in the $Ba_{1-x}Ca_x(Mg_{1/3}Nb_{2/3})O_3$ ceramics sintered at 1500 °C are illustrated in Fig. 9. In the beginning, the τ_f decreased slowly with the increasing of substitution amount of Ca^{2+} for Ba^{2+} in the range from $x=0$ to $x=0.01$. As we know, the distortion degree of oxygen octahedral in the BMN host crystal will be increasing with substitution amount of Ca^{2+} for Ba^{2+} increased, which decreased the symmetry of the crystal structure of BMN ceramics and result in the decreasing of τ_f value [31]. However, with the further increasing of substitution amount of Ca^{2+} for Ba^{2+}, the τ_f value increased quickly as for the further decreasing of the degree of oxygen octahedral distortion, which was closely related to degree of 1:2 ordering.

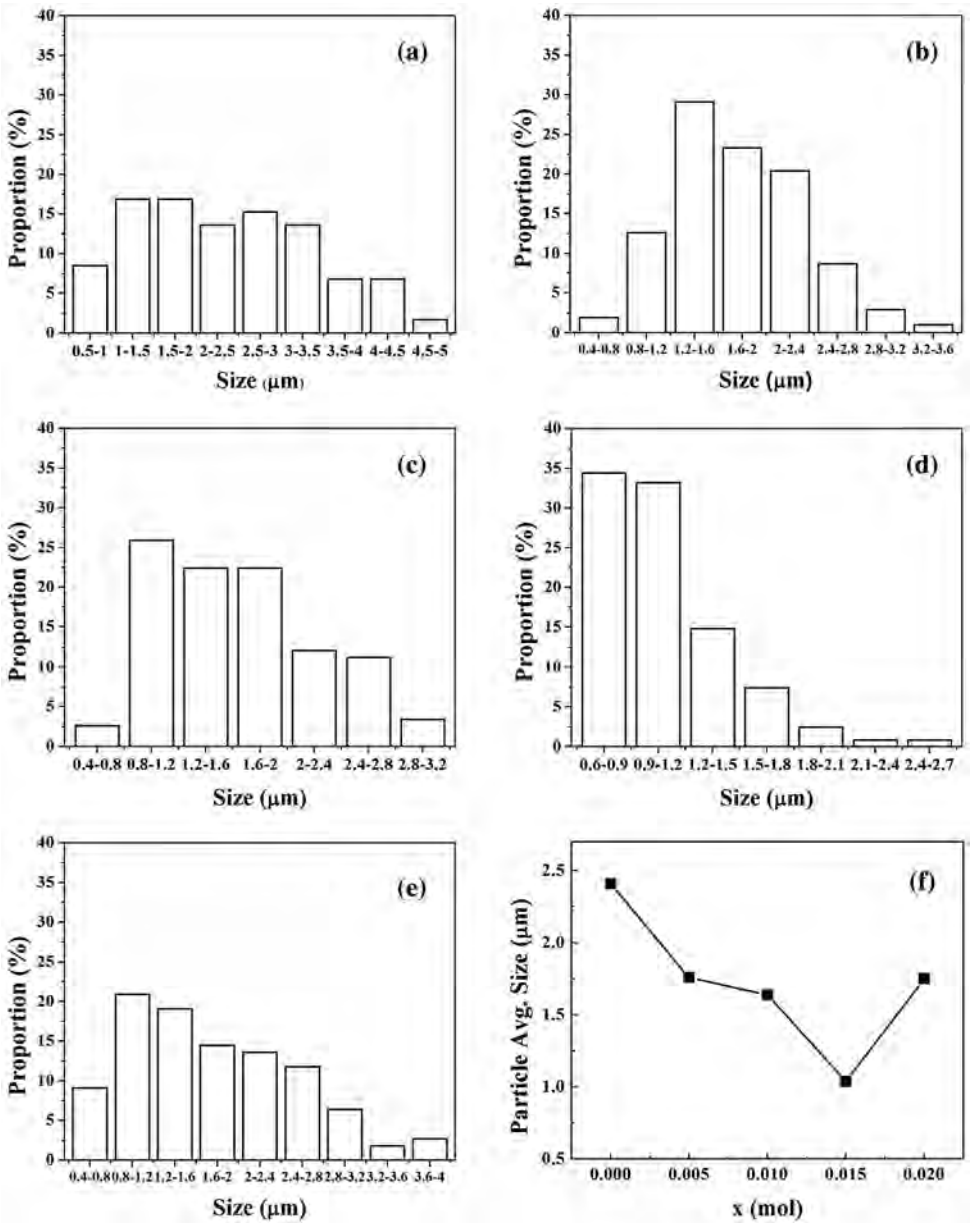

Fig. 4 Grain size distribution of $Ba_{1-x}Ca_x(Mg_{1/3}Nb_{2/3})O_3$ ceramics, corresponding to Fig. 3: **a** $x=0$, **b** $x=0.005$, **c** $x=0.01$, **d** $x=0.015$, **e** $x=0.02$; **f** grain average size

Usually, the distortion of oxygen octahedral was the major factor which influenced the behaviour of the temperature coefficient of resonant frequency (τ_f) [32–34].

4 Conclusions

In this paper, the microwave dielectric properties of $Ba_{1-x}Ca_x(Mg_{1/3}Nb_{2/3})O_3$ ceramics were revealed by XRD, SEM, Vector network analyzer and Raman spectrometer, respectively. The substitution amount of Ca^{2+} for Ba^{2+} in $Ba_{1-x}Ca_x(Mg_{1/3}Nb_{2/3})O_3$ ceramics had great influence on the degree of 1:2 ordering. The ε_r and $Q\times f$ showed strong correlation with the characters of $A_{1g}(O)$ stretch mode, including Raman shift and FWHM. The rigid oxygen octahedra revealed by Raman shift of $A_{1g}(O)$ stretch mode were related to the low dielectric constant. The ceramics with the narrowest FWHM of the $A_{1g}(O)$ stretch mode and the highest degree of 1:2 ordering achieved the highest $Q\times f$ value. The best microwave dielectric properties ($\varepsilon_r=31.64$, $Q\times f=74{,}421$ GHz, $\tau_f=14.59$ ppm/°C) of $Ba_{1-x}Ca_x(Mg_{1/3}Nb_{2/3})O_3$ ceramics were obtained while the substitution amount of Ca^{2+} for Ba^{2+} was $x=0.005$ and sintered at 1500 °C.

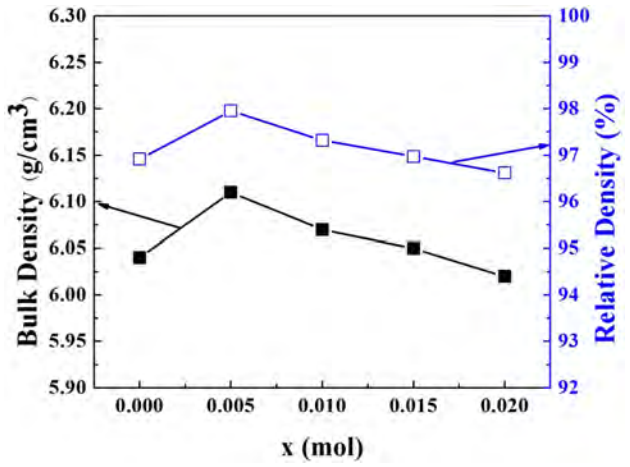

Fig. 5 The bulk density and relative density of $Ba_{1-x}Ca_x(Mg_{1/3}Nb_{2/3})O_3$ ceramics sintered at 1500 °C

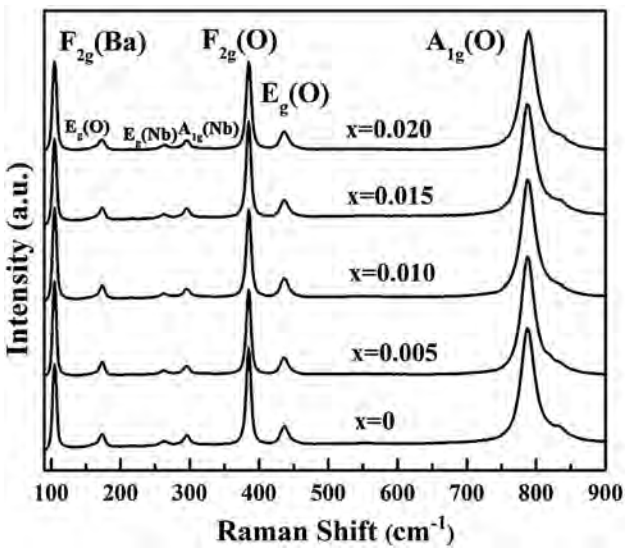

Fig. 6 The Raman spectra of $Ba_{1-x}Ca_x(Mg_{1/3}Nb_{2/3})O_3$ ceramics sintered at 1500 °C

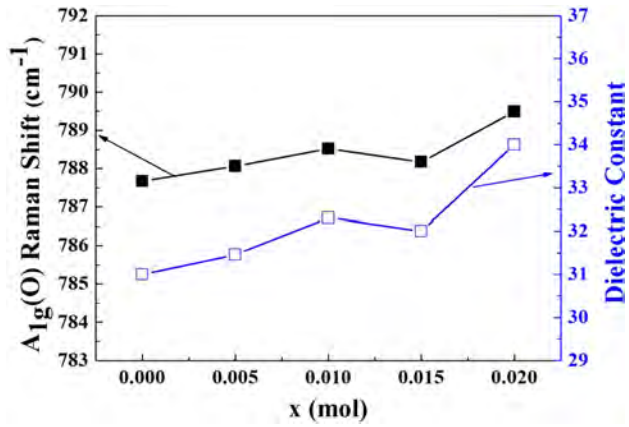

Fig. 7 The correlation of dielectric constant with FWHM of $A_{1g}(O)$ stretch mode of $Ba_{1-x}Ca_x(Mg_{1/3}Nb_{2/3})O_3$ ceramics sintered at 1500 °C

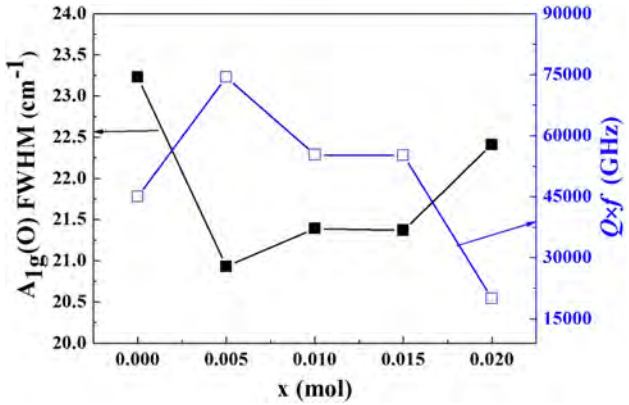

Fig. 8 The correlation of $Q \times f$ value with FWHM of $A_{1g}(O)$ stretch mode of $Ba_{1-x}Ca_x(Mg_{1/3}Nb_{2/3})O_3$ ceramics sintered at 1500 °C

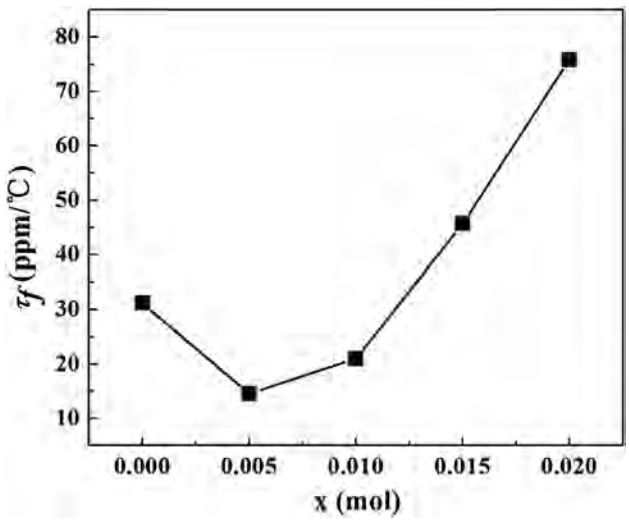

Fig. 9 The variation of τ_f in the $Ba_{1-x}Ca_x(Mg_{1/3}Nb_{2/3})O_3$ ceramics sintered at 1500 °C

Acknowledgements This work was supported by Science and Technology Projects of Jiangsu Province (BE2016050) and the Priority Academic Program Development of Jiangsu Higher Education Institutions (PAPD), Nanjing, China.

References

1. H.F. Cheng, C.T. Chia et al., Correlation of the phonon characteristics and microwave dielectric properties of the $Ba(Mg_{1/3}Ta_{2/3})O_3$ materials. J. Eur. Ceram. Soc. **27**(8), 2893–2897 (2007)
2. S. Manivannan, A. Joseph, P.K. Sharma et al., Effect of microwave and conventional sintering on densification, microstructure and dielectric properties of BZT-xCr_2O_3 ceramics. Ceram. Int. **41**(9), 10923–10933 (2015)
3. Y.W. Kim, J.H. Park, J.G. Park, Local cationic ordering behavior in $Ba(Mg_{1/3}Nb_{2/3})O_3$ ceramics. J. Eur. Ceram. Soc. **24**(6), 1775–1779 (2004)
4. C.T. Chia, Y.C. Chen, H.F. Cheng et al., Correlation of microwave dielectric properties and normal vibration modes of $xBa(Mg_{1/3}Ta_{2/3})O_3-(1-x)Ba(Mg_{1/3}Nb_{2/3})O_3$ ceramics: I. Raman spectroscopy. J. Appl. Phys. **94**(5), 3360–3364 (2003)
5. P.F. Ning, L.X. Li, P. Zhang et al., Raman scattering, electronic structure and microwave dielectric properties of $Ba([Mg_{1-x}Zn_x]_{1/3}Ta_{2/3})O_3$ ceramics. Ceram. Int. **38**(2), 1391–1398 (2012)
6. S. Nomura, Ceramics for microwave dielectric resonator. Ferroelectrics **49**(1), 61–70 (1983)
7. H. Tamura, T. Konoike, Y. Sakabe et al., Improved high-*Q* dielectric resonator with complex perovskite structure. J. Am. Ceram. Soc. **67**(4), c59–c61 (1984)
8. H.J. Lee, H.M. Park, H. Ryu et al., Microstructural changes in lanthanum-doped barium magnesium niobate. J. Am. Ceram. Soc. **82**(9), 2529–2537 (1999)
9. M.A. Akbas et al., Structure and dielectric properties of the $Ba(Mg_{1/3}Nb_{2/3})O_3$-$La(Mg_{2/3}Nb_{1/3})O_3$ system. J. Am. Ceram. Soc. **8**(8), 2205–2208 (2010)
10. H. Zhang, C. Diao, S. Liu et al., XRD and Raman study on crystal structures and dielectric properties of $Ba[Mg_{(1-x)/3}Zr_xNb_{2(1-x)/3}]O_3$ solid solutions. Ceram. Int. **40**(1), 2427–2434 (2014)
11. Z.Q. Tian, H.X. Liu, H.T. Yu et al., Effect of $BaWO_4$ on microstructure microwave dielectric properties of $Ba(Mg_{1/3}Nb_{2/3})O_3$. Mater. Chem. Phys. **86**(1), 228–232 (2004)
12. Y. Bisht, R. Tomar, P. Abhilash et al., Microwave dielectrics: solid solution, ordering and microwave dielectric properties of $(1-x)Ba(Mg_{1/3}Nb_{2/3})O_3$-$xBa(Mg_{1/8}Nb_{3/4})O_3$ ceramics. Bull. Mater. Sci. **40**(6), 1165–1170 (2017)
13. C.T. Lee, Y.C. Lin, C.Y. Huang, C.Y. Su, C.L. Hu, Cation ordering and dielectric characteristics in barium zinc niobate. J. Am. Ceram. Soc. **90**(2), 483–489 (2007)
14. M. Bieringer, S.M. Moussa, L.D. Noailles et al., Cation ordering, domain growth, and zinc loss in the microwave dielectric oxide $Ba_3ZnTa_2O_{9-\delta}$. Chem. Mater. **15**(2), 586–597 (2003)
15. Y. Yang, R. Fu, S. Agathopoulos et al., Influence of the processing way for La^{3+}-doping on crystal structure, microstructure, and microwave dielectric properties of $Ca_{0.7}Ti_{0.7}La_{0.3}Al_{0.3}O_3$ ceramics. Ceram. Int. **42**(16), 18108–18115 (2016)
16. B.W. Hakki, P.D. Coleman, A dielectric resonator method of measuring inductive capacities in the millimeter range. IRE Trans. Microw. Theory Tech. **8**(4), 402–410 (1960)
17. W.E. Courtney, Analysis and evaluation of a method of measuring the complex permittivity and permeability microwave insulators. IEEE Trans. Microw. Theory Tech **18**(8), 476–485 (1970)
18. M.S. Fu, X.Q. Liu, X.M. Chen, Y.W. Zeng, Effects of Mg substitution on microstructures and microwave dielectric properties of $Ba(Zn_{1/3}Nb_{2/3})O_3$ perovskite ceramics. J. Am. Ceram. Soc. **93**(3), 787–795 (2010)
19. Y.X. Shi, J. Shen, J. Zhou et al., Structure and optical properties of Sn^{4+} doped $Ba(Mg_{1/3}Nb_{2/3})O_3$ transparent ceramics. Ceram. Int. **41**, 253–257 (2015)
20. S. Nomura, The effect of Mg deficiency on the microwave dielectric properties of $Ba(Mg_{1/3}Nb_{2/3})O_3$ ceramics. J. Mater. Sci. Lett. **17**(20), 1777–1780 (1998)
21. B.K. Kim, H.O. Hamaguchi, I.T. Kim et al., Probing of 1:2 ordering in $Ba(Ni_{1/3}Nb_{2/3})O_3$ and $Ba(Zn_{1/3}Nb_{2/3})O_3$ ceramics by XRD and Raman spectroscopy. J. Am. Ceram. Soc. **78**(11), 3117–3120 (1995)
22. R.D. Shannon, Revised effective ionic radii and systematic studies of interatomic distances in halides and chalcogenides. Acta Crystallogr. A **32**(1), 751–767 (1976)
23. P.P. Ma, H. Gu, X.M. Chen, Evaluation of the 1:2 ordered structure of $Ba(B'_{1/3}B''_{2/3})O_3$ perovskites along various zone axes using transmission electron microscopy. J. Mater. Chem. C **3**(41), 10755–10760 (2015)
24. J.F. Li, A. Kawasaki, R. Watanabe, Hot isostatically pressed SiC-AlN powder mixtures: effect of milling on solid-solution formation and related properties. J. Am. Ceram. Soc. **81**(6), 1445–1452 (2005)
25. H.J. Lee, H.M. Park, K.C. Yang et al., Microstructural observations in barium calcium magnesium niobate. J. Am. Ceram. Soc. **83**(9), 2267–2272 (2010)
26. I.G. Siny, R.W. Tao, R.S. Katiyar et al., Raman spectroscopy of Mg-Ta order-disorder in $Ba(Mg_{1/3}Ta_{2/3})O_3$. J. Phys. Chem. Solids **59**(2), 181–195 (1998)
27. Z. Wang, B. Huang, L. Wang et al., Low loss $(Ba_{1-x}Sr_x)(Co_{1/3}Nb_{2/3})O_3$ solid solution: phase evolution, microstructure and microwave dielectric properties. J. Mater. Sci. Mater. Electron. **26**(6), 4273–4279 (2015)
28. C.T. Lee, C.Y. Huang, Y.C. Lin et al., Structural and dielectric characteristics in a $Ca(Mg_{1/3}Nb_{2/3})O_3$-$CaZrO_3$ system. J. Am. Ceram. Soc. **90**(10), 3148–3155 (2007)
29. Q. Liao, Y. Wang, J. Feng et al., Ultra-low fire glass-free $Li_3FeMo_3O_{12}$ microwave dielectric ceramics. J. Am. Ceram. Soc. **97**(8), 2394–2396 (2014)
30. M.Y. Chen, C.T. Chia, I.N. Lin et al., Microwave properties of $Ba(Mg_{1/3}Ta_{2/3})O_3$, $Ba(Mg_{1/3}Nb_{2/3})O_3$ and $Ba(Co_{1/3}Nb_{2/3})O_3$ ceramics revealed by Raman scattering. J. Eur. Ceram. Soc. **26**(10–11), 1965–1968 (2006)
31. H.J. Lee, H.M. Park, Y.W. Song et al., Microstructure and dielectric properties of barium strontium magnesium niobate. J. Am. Ceram. Soc. **84**(9), 2105–2110 (2001)
32. J.H. Paik, S.K. Kim, M.J. Lee et al., Ordering structure of barium magnesium niobate ceramic with A-site substitution. J. Eur. Ceram. Soc. **26**(14), 2885–2888 (2006)
33. E.L. Colla, I.M. Reaney et al., Effect of structural-changes in complex perovskites on the temperature-coefficient of the relative permittivity. J. Appl. Phys. **74**(5), 3414–3425 (1993)
34. E.L. Colla, I.M. Reaney, N. Setter, The temperature coefficient of the relative permittivity of complex perovskites and its relation to structural transformations. Ferroelectrics **133**(1), 217–222 (1992)